Dimitrios G. Lignos
Alexander R. Hartloper

Steel column stability and implications in seismic assessment of steel structures according to Eurocode 8 Part 3

Seismic performance assessment of new and existing steel structures based on nonlinear static (pushover) analysis necessitates the use of engineering-oriented models that trace the nonlinear response of structural steel elements under seismic and static loading. Recent experiments and corroborating finite element simulations on I- and H-shaped steel columns constitute an important data source for such a development. This paper presents important insights regarding the behaviour of steel columns under cyclic and monotonic loading based on an assembled steel column database. We propose simple, yet accurate, practice-oriented models to predict the strength and deformation capacities at yield and ultimate rotations (near collapse) of steel columns within the framework of Eurocode 8 Part 3 (EC8-Part 3). The proposed models are derived based on first principles of mechanics along with robust statistical approaches leveraging the assembled datasets. It is shown that the current EC8-Part 3 modelling provisions for steel columns do not reflect the column behavioural trends from the available databases. The influence of loading history on the derived modelling recommendations for columns is also quantified and discussed. The proposed recommendations may be incorporated in future versions of EC8-Part 3 for seismic performance assessment of new and existing steel structures.

Keywords Steel columns, seismic stability, near collapse limit state, local buckling, plastic rotation capacity, seismic assessment, pushover analysis, steel structures

Stabilität der Stahlsäule und Auswirkungen auf die seismische Bewertung von Stahlkonstruktionen nach Eurocode 8 Teil 3. Die seismische Leistungsbewertung neuer und bestehender Stahlkonstruktionen auf der Grundlage einer nichtlinearen statischen (Pushover-) Analyse erfordert die Verwendung konstruktionsorientierter Modelle, die das nichtlineare Verhalten von Stahlbauteilen unter seismischer und statischer Belastung nachzeichnen. Neuere Experimente und bestätigende Finite-Elemente-Simulationen an I- und H-förmigen Stahlsäulen sind eine wichtige Datenquelle für eine solche Entwicklung. In diesem Artikel werden wichtige Erkenntnisse zum Verhalten von Stahlsäulen unter zyklischer und monotoner

Belastung anhand einer zusammengestellten Stahlsäulendatenbank vorgestellt. Wir schlagen einfache, aber genaue, praxisorientierte Modelle vor, um die Festigkeits- und Deformationskapazitäten bei Streckgrenze Rotation und Rotationsvermögen (nahezu Kollaps) von Stahlsäulen im Rahmen von Eurocode 8 Teil 3 (EC8-Teil 3) vorherzusagen. Die vorgeschlagenen Modelle basieren auf Grundprinzipien der Mechanik sowie auf robusten statistischen Ansätzen unter Verwendung der zusammengestellten Datensätze. Es wird gezeigt, dass die aktuellen Modellierungsbestimmungen für Stahlsäulen nach EC8-Teil 3 nicht die Trends des Säulenverhaltens widerspiegeln, die aus den verfügbaren Datenbanken hervorgehen. Der Einfluss der Beanspruchungsgeschichte auf die abgeleiteten Modellierungsempfehlungen für Säulen wird ebenfalls quantifiziert und diskutiert. Die vorgeschlagenen Empfehlungen können in zukünftige Versionen von EC8-Teil 3 zur Bewertung der seismischen Leistungsfähigkeit neuer und bestehender Stahlkonstruktionen aufgenommen werden.

1 Introduction

In the context of performance-based seismic assessment of new and existing steel structures, the engineering profession often uses nonlinear static (so-called pushover) and dynamic analysis procedures. Nonlinear structural analysis is also deployed within risk-targeted frameworks [1]–[3] to deduce realistic values of the behaviour factor, q as well as the overstrength factor, Ω (e.g., Elkady and Lignos [4]), of earthquake-resistant structural systems according to various seismic design standards. Nonlinear analysis requires the reliable quantification of the strength and ductility of structural members undergoing cyclic loading. In the US, the current state-of-practice in nonlinear structural modelling and analysis guidelines is ASCE 41 [5], which was formerly known as FEMA 356 [6]; whereas in Europe, complementary guidelines have been incorporated in Eurocode 8 Part 3 (EC8-Part 3) [7] with emphasis at yield and ultimate deformation capacities of structural members. Within EC8-Part 3, while the above nonlinear modelling guidelines for reinforced concrete members are well established [8], the corresponding ones for steel members are fairly limited. Albeit for steel and composite beams this has been recently addressed [9], [10] including theoretical expressions that rely on moment curvature analysis [11]–[13], a fundamental gap still prevails for I- and H-shaped steel columns, thereby prohibiting (a) optimal interventions in existing steel structures; (b) the full potential of steel in prospective building seismic designs.

The above limitations were attributed to the lack of available experimental data manifesting the deformation capacity of steel columns under cyclic loading. In recent years, experiments have

been conducted to address this pressing concern [14]–[19]. It is also worth stating that concurrent continuum finite element (CFE) analyses [20], [21] have been carried out to complement the experimental data and to expand the behavioural insights for a broad range of steel column geometries.

The available experimental data and corroborating CFE analysis results constitute a valuable resource for calibration of practice-oriented nonlinear models that prognosticate the nonlinear behaviour of steel columns. With this in mind, a large experimental and simulated dataset was assembled and exploited herein for the development of engineering-oriented models to estimate the strength and deformation capacities of steel columns at yield and ultimate. The derived models are established on the basis of mechanics principles along with statistical (or empirical) approaches. The proposed models may be fully utilized in nonlinear static (pushover) analyses within the framework of EC8-Part 3 [7] for the seismic assessment of new and existing steel structures.

2 Steel column hysteretic response, performance indicators and review of assembled database

This section provides an overview of the complex hysteretic behaviour of steel columns under multiaxial cyclic loading. It also discusses the physical aspects of column response and the moment-rotation curves to establish a context, in which the assembled dataset (experiments and CFE results) can be interpreted to address the primary scope of this paper.

2.1 Steel column behaviour under monotonic and cyclic loading

Steel columns in earthquake-resistant lateral load resisting systems experience lateral drift demands coupled with either constant compressive or variable axial load demands. The former is common in interior columns, whereas the latter is typical in exterior (end) columns due to transient overturning effects. Figure 1 depicts the monotonic and symmetric cyclic behaviour of two nominally identical interior cantilever steel columns in terms of moment – chord rotation, θ, (see Figure 1a) and column axial shortening, δ_{axial}, versus θ (see Figure 1b). The chord rotation, θ, refers to the rotation of the member of its entire length, L. This is equivalent to the storey drift ratio in this case. While interior steel columns under monotonic loading experience local buckling only at their compressive flange (see Figure 1c), their hysteretic behaviour under symmetric cyclic loading is characterized by symmetric local buckling on both flanges (see Figures 1d).

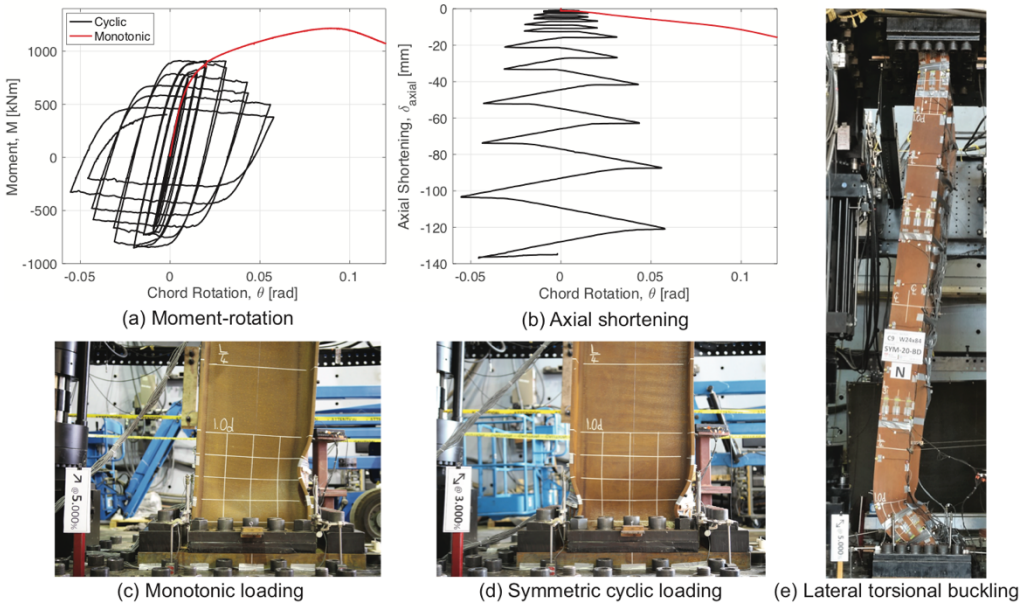

Figure 1 Typical hysteretic behaviour of steel columns under monotonic and cyclic loading – data and images from Elkady and Lignos [15], [18] and Cravero et al. [19]

Depending on the member slenderness ratio, L_b/i_z (L_b is the unbraced length of the column; i_z is the radius of gyration with respect to the weak axis of the steel cross-section), the local buckling progression may be coupled with inelastic lateral torsional buckling [16], [18] at storey drift demands representative of significant damage (SD) limit states (see Figure 1e). Evidently, column axial shortening is a common instability mode observed in fixed-end columns due to the progression of nonlinear local and member geometric instabilities under lateral loading. Note that in today's capacity design principles [22] we do not encounter such an instability mode in first storey fixed end columns of steel moment-resisting frame systems. However, this is an important design consideration. Research by the first author [15], [23] has highlighted that during an earthquake adjacent first storey steel columns in moment-resisting frame systems may exhibit differential axial shortening due to differences in the imposed column axial load demands. In turn, this may cause slab tilting and subsequently catenary action in steel girders as part of full-strength beam-to-column connections. This issue deserves more attention in future studies associated with the collapse prevention of steel moment-resisting frame systems under earthquake loading.

2.2 Steel column performance indicators

Of interest herein are the deformation capacities of steel columns at yield, θ_y, and ultimate, θ_u, as shown in Figure 2. The former may be prevalent for damage states associated with modest

lateral drift demands (e.g., design-basis earthquake event) in which repairability in the aftermath of earthquakes is imperative. The latter may be relevant in seismic performance assessments of new and existing steel structures near the collapse (NC) limit state. Hereinafter, θ_u, refers to the chord rotation at which a steel column has lost 20% of its peak flexural resistance. This is analogous with prior related efforts [8] to characterize the deformation capacities of reinforced concrete members within the framework of EC8-Part 3.

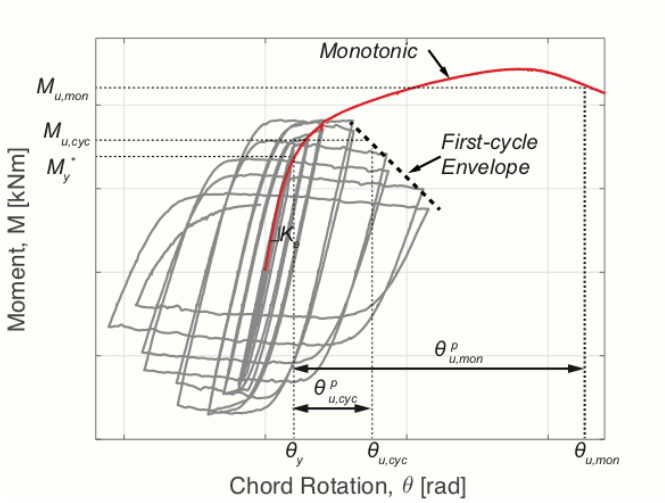

Figure 2 Column performance indicators for seismic assessment of steel structures based on nonlinear static analysis

Referring to Figure 2, the yield point (θ_y, M_y^*) and the elastic rotational stiffness, K_e, of the member are the same for both monotonic and cyclic loading, whereas the point at ultimate (θ_u, M_u) is defined separately for monotonic and cyclic loading. Referring to Figure 2, the effective yield moment, M_y^*, is defined at the intersection of the straight lines joining the elastic rotational stiffness of a column and that connecting (θ_y, M_y^*) with (θ_u, M_u). The latter is defined based on the equal area rule. The effective yield point can be deduced by first principles of mechanics, whereas the ultimate point may be computed based on empirical formulations proposed herein for the plastic rotation, $\theta^p_{u,mon}$ $(\theta^p_{u,cyc})$, from yield to ultimate. Vis-à-vis the above discussion, the column performance indicators are identified based on available experimental and simulated data discussed in Sections 2.3 and 2.4, respectively.

2.3 Available experimental data

The experimental database used herein comprises 158 tests of steel columns mostly under uniaxial bending coupled with constant and variable axial load demands. Twenty-one tests were conducted under biaxial bending. The test specimens including their basic loading parameters

and a complete list of references are summarized in Table 1. The significant majority of the column cross-sections feature Class 1 to 3 cross-sections according to [24] compactness limits. A handful of test specimens are comprised of Class 4 cross-sections.

Table. 1 Available experimental data on steel columns under monotonic and cyclic loading

Study	Number of tests	Axial load ratio, v	Lateral loading protocol
[25]	6	0,30 – 0,80	Symmetric Cyclic
[26]	10	0 – 0,80	Symmetric Cyclic
[27]	42	0 – 0,75	Monotonic
[28]	9	0,30 – 0,70	Symmetric Cyclic
[29]	6	0,15 – 0,30	Symmetric Cyclic
[30]	9	0,15 – 0,30	Symmetric Cyclic
[31]	17	0,20 – 0,50	Symmetric Cyclic
[15]	12	0,15 – 0,50	Monotonic, Symmetric Cyclic, Collapse-Consistent
[16]	24	0 – 0,50	Symmetric Cyclic
[18]	10	0,20 – 0,50	Symmetric Cyclic, Collapse-Consistent
[19]	12	0,30 – 0,75	Monotonic, Symmetric Cyclic, Collapse-Consistent

Most specimens were of conventional cantilever type or had fixed-end boundary conditions. Ten specimens tested with fixed-flexible boundary conditions reflecting actual boundary conditions of a first storey steel column within a moment-resisting frame. While the significant majority of available physical tests constitutes specimens subjected to a routinely used symmetric cyclic loading protocol [32], thirteen tests were subjected to collapse-consistent cyclic loading histories [33] representing the ratcheting behaviour of steel columns prior to incipient collapse [34], [35]. In 49 tests, the imposed lateral load was monotonic. While the hysteretic response indicated flexural yielding in all specimens, several specimens did not reach the rotation at ultimate, θ_u, as indicated in Section 2.2.

In brief, the axial load ratio, $v = N/N_{pl}$ of the collected test specimens (where, N is the imposed compressive axial load demand and $N_{pl} = f_y A$, is the reference axial strength of a steel column deduced by its nominal yield stress, f_y, times its cross-sectional area, A) ranges from 0 to 0,75. The geometry of the test specimens in the database in terms of local web slenderness ratio,

h_1/t_w (h_1 is the web clear height between the inner radii and t_w is the web thickness) ranges from 6 to 90, whereas that of the member slenderness ratio, L_b/i_z ranges from 13 to 160. To populate the experimental dataset to cover the entire range of column cross-sections used in the current seismic design practice, available virtual tests were also collected from continuum CFE analyses conducted by the first author and his former students [21]. This set of data is described in the subsequent section.

2.4 Available simulated data from continuum nonlinear finite element analyses

The virtual test matrix to populate the experimental database discussed in Section 2.3 is developed on the basis of CFE simulations based on rigorous nonlinear modelling procedures outlined in Elkady and Lignos [20], [21]. In brief, multiaxial material plasticity is considered based on the Voce and Chaboche material model [36]–[38]. The input material model parameters have been calibrated as discussed in [39], [40] to tackle the challenge of non-uniqueness [41]. Residual stresses are explicitly considered in the CFE simulations according to Young's distributions [42]. These were found to be realistic based on recent residual stress measurements [43]. Finally, member and local geometric nonlinearities in the CFE models are triggered based on buckling analysis of representative buckling modes of the respective column member. The imperfection amplitudes were found to be $L/1500$, $b/250$ and $h_1/250$ for the global and local buckling modes, respectively. Note that the above imperfections are within the product qualification limits according to [44]. Figure 3 illustrates the successful representation of physical tests under monotonic and cyclic loading based on the CFE models suggesting confidence to the simulated predictions.

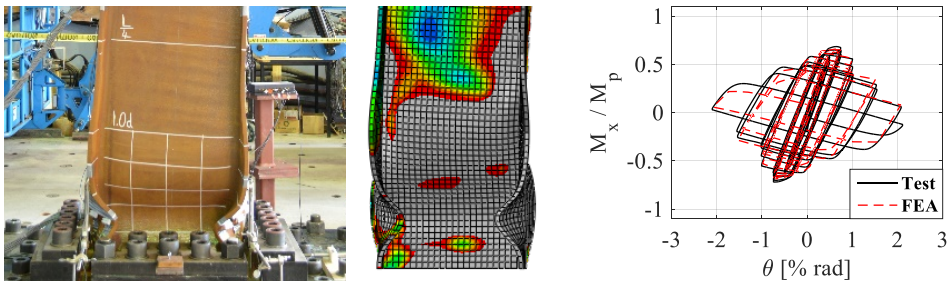

Figure 3 Representative illustrations of validated continuum finite element analyses of steel columns under cyclic loading (image and data from Elkady and Lignos [18], [21])

The virtual test matrix, which is made publicly available from the authors in the Zenodo data repository for reuse, provides a considerable expansion of the available experimental data to cover all possible column cross-sections that could be used in seismic building designs.

3 Steel column behavioural trends and discussion

The emphasis herein is on the deduced column parameter indicators from the moment-rotation relations of the available experimental and simulated data discussed in Sections 2.3 and 2.4, respectively. A distinction is made between monotonic and cyclic data, if necessary, particularly for the corresponding flexural strength, M_u and rotation at ultimate, θ_u. The observed trends, discussion and modelling recommendations are based on a synthesis from the two databases discussed earlier.

3.1 Elastic rotational stiffness, K_e

The elastic rotational stiffness of a steel member under combined actions constitute the flexural, shear and axial components. Elastic axial deformations may be disregarded for steel columns under lateral loading, therefore, the chord rotation, θ, of a steel column over its length, L, is defined based on the principle of virtual work,

$$\theta = \delta/L \cong \frac{1}{L}\left(\int_0^L \frac{M\overline{M}}{EI}dx + \int_0^L \frac{V\overline{V}}{GA}dx\right) \tag{1}$$

where, E is the Young's modulus; I is the cross-sectional moment of inertia with respect to the axis of bending; G is the shear modulus of the steel material; and A is the shear area of the respective column cross-section. For a I-shape column with length L and any type of boundary conditions under lateral load, Eq. (1) ultimately yields to the following expression the elastic rotational stiffness, K_e,

$$K_e = \frac{1}{1/K_{flexure} + 1/K_{shear}} \tag{2}$$

$$K_{flexure} = \frac{a_1 EI}{L} \tag{3}$$

and,

$$K_{shear} = \begin{cases} \dfrac{GA(a_2 L)}{0{,}85 + 2{,}32\, bt_f/ht_w}, & strong-axis\ bending \\ \dfrac{G(2bt_f)(a_2 L)}{1{,}2}, & weak-axis\ bending \end{cases} \tag{4}$$

Equation (4) has been developed for I-shape cross-sections according to Cowper [45]. Where, E, G are the Young and shear modulus of the steel material, respectively; b, t_f, t_w, h are the flange width, flange thickness, web thickness and full depth, respectively, of the I-shape cross-

section; a_1 and a_2 are parameters that depend on the member end boundary conditions. Particularly, a_1=3 and a_2=1 for a cantilever column; a_1=6 and a_2=0,5 for a member in contraflexure.

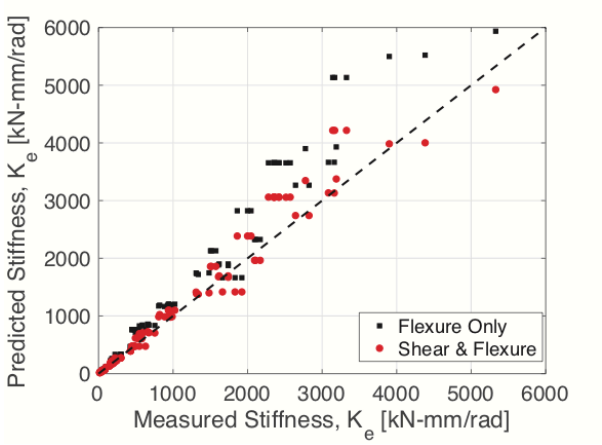

Figure 4 Measured versus predicted elastic rotational stiffness of I- and H-shaped steel columns

Figure 4 illustrates the measured K_e from all available experiments versus the computed one from engineering mechanics first principles. There is a perception that the shear contribution to K_e, of I-shape members under lateral loading is negligible. Referring to Figure 4, the predicted rotational stiffness for all the collected test specimens is estimated based on flexure only (Eq. 3) as well as combined flexure and shear (Eq. 2). On average, the elastic stiffness of I-shape steel columns is underestimated by about 20% when shear deformations are neglected. The largest errors in the predicted K_e values are usually observed in columns with either deep cross-sections ($h \geq 400mm$) or stocky ones ($t_f \geq 35mm$). Therefore, Eq. (2) is generally recommended in order to compute K_e of steel columns within the framework of EC8-Part 3.

3.2 Column flexural resistance at yield

The effective flexural resistance, M_y^*, of steel columns is highly dependent on the applied compressive axial load ratio, v, due to the axial load-flexure interaction. Figure 5 illustrates a comparison of all the $N - M$ pairs at the cross-sectional level from the experimental database. The EC3-Part 1 [24] and AISC-360-16 [46] flexure-axial load interaction curves are also superimposed. According to [46],

$$M = \begin{cases} M_c \cdot \left(1 - \frac{1}{2}v\right), & v < 0{,}20 \\ \frac{9}{8} \cdot M_c \cdot (1 - v), & v \geq 0{,}20 \end{cases} \quad (5)$$

Where, M_c, is the flexural resistance of a steel column based on the plastic section modulus,

W_{ply}, for Class 1 and 2 cross-sections or the elastic section modulus, W_{ely}, for Class 3 cross-sections. Flexural buckling (member level) is not considered in this comparison since none of the test specimens exhibited this failure mode. In the horizontal axis, the flexural resistance, M_y^* is normalized with respect to M_c. Generally, both interaction curves trace reasonably well the onset of flexural yielding of columns. Unlike the AISC-360-16 interaction curve, the EC3-Part 1 interaction curve suggests no flexural strength reduction when, $\nu \leq 0{,}25$. This is not justified based on the available experimental data.

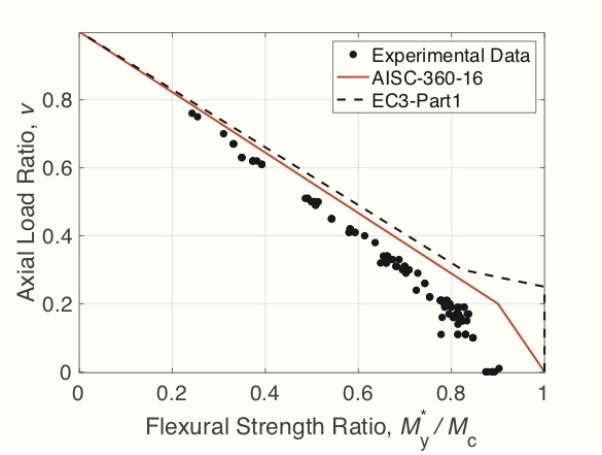

Figure 5 Comparison of test data with flexure-axial load interaction curves

For the purposes of seismic assessment of new and existing steel structures, the steel material overstrength parameter, γ_{ov}, should be considered in the computation of M_y^* for steel columns. While the current EC8-Part 1 [22] suggests a fixed value of 1,25 for γ_{ov}, the corresponding values suggested from the OPUS program [47] are recommended. Depending on the employed steel material, a different value of γ_{ov} is suggested for a more reliable estimation of M_y^*.

3.3 Chord rotation of steel columns at yielding

Figure 6 depicts the dependence of the steel column chord rotation at yielding, θ_y, with respect to the shear span ratio, L_o/h (see Figure 6a), the web slenderness ratio, h_1/t_w (see Figure 6b) and the imposed compressive axial load ratio, ν (see Figure 6c). The assessment is based on the experimental dataset only. Referring to Figure 6a, there is a dependency between θ_y and L_o/h. Longer column members tend to have a larger elastic deflection prior to yielding compared to shorter ones with the same cross-sectional depth. Equation (2) explicitly captures the effect of L_o/h on θ_y. On the other hand, Figure 6b suggests that there is no evident dependence of h_1/t_w on θ_y. The observed variability at particular h_1/t_w ratios is mostly attributed to the imposed

compressive axial load ratio. Figure 6c, shows the identified θ_y values for each test specimen versus the corresponding v. The higher the imposed compressive axial load ratio the smaller the yield rotation of a steel column. This is mostly attributed to the influence of v on the flexural resistance of a column cross-section (see Section 3.2). It is found that θ_y may be computed based on Eq. (6),

$$\theta_y = \frac{M_y^*}{K_e} \tag{6}$$

Where, M_y^* is the column flexural resistance reduced by the effects of v based on the AISC-360-16 design provisions as discussed in Section 3.2; and K_e may be computed according to Eq. (2).

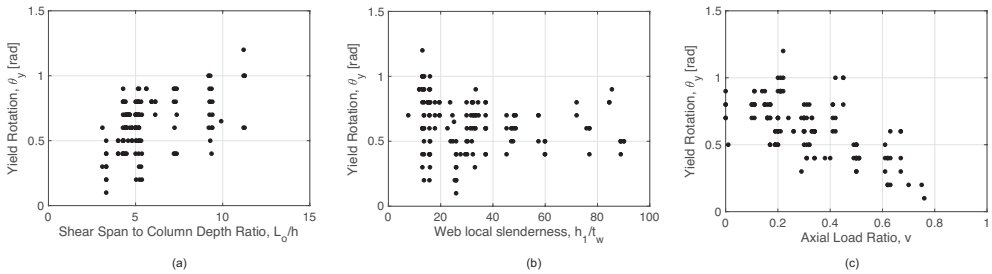

Figure 6 Yield rotation of steel columns as a function of geometric and loading parameters; (a) shear span to column depth ratio; (b) web local slenderness ratio; (c) axial load ratio

3.4 Ultimate chord rotation of steel columns

With regards to the ultimate chord rotation, θ_u, of steel columns, the complete dataset (experimental and simulated) is utilized to facilitate the discussion herein. The reason is that about 50% of the assembled experimental data did not reach θ_u. Referring to Figure 2, θ_u may be computed as follows,

$$\theta_u = \theta_y + \theta_u^p \tag{7}$$

Unlike, reinforced concrete members, it is preferred to express the ductility of steel columns as a function of the plastic rotation, θ_u^p from the yield to the ultimate chord rotation. One reason is that θ_y can be directly computed based on first principles of mechanics. Moreover, the dependence of a column's inelastic deformation beyond yielding on L_b/i_z is lost, since the axial load ratio dominates the cyclic response. Prior related studies [10], [34] found that when the plastic deformation of a steel member is isolated, it is generally regarded to be a more stable parameter than the chord rotation at ultimate. Therefore, the discussion herein focuses on θ_u^p.

Figure 7 illustrates the primary geometric and loading parameters influencing $\theta_{u,cyc}^p$ for

symmetric cyclic loading. In particular, Figure 7a suggests that column cross-sections with Class 3 webs ($h/t_w \geq 40$) typically achieve a $\theta^p_{u,cyc}$ of 2% rad (i.e., $\theta_{u,cyc} \geq 2{,}5\%\, rad$) for imposed compressive axial load ratios of 0,30 or less, which is the expected axial load range in columns of steel moment-resisting frame systems [33] and the maximum allowable according to [22] (see section 6.3.1(2)). Therefore, the use of cross-sections with Class 3 webs in prospective steel MRF designs in European regions of moderate seismicity may suffice. Similarly, column cross-sections with Class 1 webs are able to achieve a $\theta^p_{u,cyc}$ of 3,5% rad (i.e., $\theta_{u,cyc} \geq 4{,}0\%\, rad$), which matches the established targets for prequalified dissipative beam-to-column connections [48].

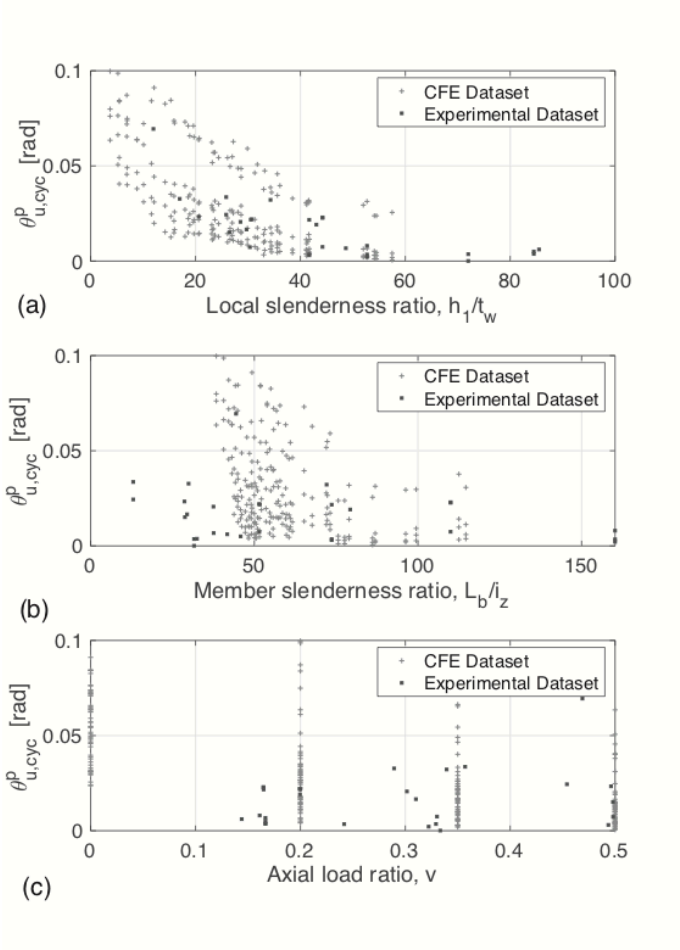

Figure 7 Dependence of plastic rotation at ultimate, $\boldsymbol{\theta^p_{u,cyc}}$, on geometric and loading parameters of a steel column under symmetric cyclic loading; (a) local web slenderness ratio; (b) member slenderness ratio; (c) axial load ratio

Referring to Figure 7b, there is an apparent dependence of $\theta^p_{u,cyc}$ to L_b/i_z. The datasets suggest that members with $L_b/i_z \geq 70$ do not generally exhibit a plastic rotation of more than 1,5% rad. This is due to coupling of plastic lateral torsional buckling with local buckling [18], [21]. This typically occurs at inelastic chord rotations larger than 2,0% rad. Finally, Figure 7c highlights

the predominant effect of the imposed axial load ratio on $\theta_{u,cyc}^{p}$. While columns with $v \leq 0{,}30$ seem to exhibit appreciable ductility for seismic resistant design, the ones with a $v \geq 0{,}60$ have fairly limited plastic rotation capacity; hence they may be treated as force – controlled elements (i.e., zero ductility) with regards to seismic assessment of steel structures. The above trends are general and reflect findings for monotonic loading as well. The dependence of θ_u^p on E/f_y (modulus of elasticity-to-yield stress ratio) is of secondary importance. The interrelation of the above geometric and loading variables and their influence on θ_u^p is depicted by multivariate empirical expressions developed and presented in the next section.

4 Empirical expressions for the flexural strength and chord rotation of steel columns at ultimate

This section discusses the development of empirical expressions for the estimation of the flexural strength, M_u, and plastic rotation, θ_u^p of I- and H-shaped steel columns from the yield to the ultimate chord rotation within the framework of EC8-Part 3. Two types of expressions are developed. One for monotonic and one for reversed cyclic loading. The database of simulated results is used as a training set for the development of the multivariate regression equations, whereas the experimental database is used as a validation set. The proposed empirical equations with regards to M_u and θ_u^p are developed based on the following multiple regression model,

$$y = \beta_o \left(\frac{h_1}{t_w}\right)^{b_1} \cdot \left(\frac{L_b}{i_z}\right)^{b_2} \cdot (1 - v_G)^{b_3} + \varepsilon \tag{8}$$

Where, y is either θ_u^p or M_u/M_y^*; β_j are regression coefficients; and ε is the error between the test and predicted responses. Notice that the gravity-induced component of axial load ratio, $v_G = N_G/N_{pl}$, is used in the subsequent regressions. Research ([15], [19], [28], [49]) suggests that this is a more rational value to be used than the absolute maximum axial load ratio, v, which includes the transient axial load component. The coefficient of variation (COV) as well as the coefficient of determination, R^2, are utilized to measure the goodness-of-fit. The reported *COV* values are important since they provide a sense of the expected uncertainty in the predictors. The selected predictors have been found to be statistically significant to θ_u^p and M_u/M_y^* based on a standard *t*-test. While CFE simulations generally reveal reliable predictions, because there is no experimental evidence on plastic rotations from yield to ultimate above 0,15rad, a limit of $\theta_u^p \leq 0{,}15rad$ is imposed, following a standard practice in similar efforts [49], [50]. Similarly, a limit

of $M_u/M_y^* \leq 1{,}2$ is considered for very stocky cross-sections that tend to harden considerably under cyclic/monotonic loading.

4.1 Monotonic loading

The plastic rotation, $\theta_{u,mon}^p$ and the corresponding flexural strength $M_{u,mon}$ of a steel column under monotonic loading may be computed as follows,

$$\frac{M_{u,mon}}{M_y^*} = 10{,}0\left(\frac{h_1}{t_w}\right)^{-0{,}2} \cdot \left(\frac{L_b}{i_z}\right)^{-0{,}4} \cdot (1-v_G)^{0{,}4} \leq 1{,}2 \quad (9)$$

$(R^2 = 0{,}76, COV = 0{,}10,\ N = 160 \text{ points})$

$$\theta_{u,mon}^p = 296{,}75\left(\frac{h_1}{t_w}\right)^{-1{,}4} \cdot \left(\frac{L_b}{i_z}\right)^{-0{,}8} \cdot (1-v_G)^{2{,}7} \leq 0{,}15rad \quad (10)$$

$(R^2 = 0{,}91, COV = 0{,}32, N = 160 \text{ points})$

The above equations are valid within the following range of parameters, $12 < h_1/t_w < 58$; $43 \leq L_b/i_z \leq 115$; $0 \leq v_G \leq 0{,}50$. Note that column cross-sections with $h_1/t_w < 12$ where not considered in the statistical analysis because they did not reveal any flexural strength deterioration even at chord rotations of 0,20rads or higher. This is to be expected for such stocky profiles [28], [33]. However, in this case fracture of complete joint penetration groove welds between the steel profile and the corresponding column base are likely to control the plastic deformation capacity of the member at high inelastic straining.

4.2 Cyclic loading

With regards to cyclic loading, the plastic rotation, $\theta_{u,cyc}^p$ and the flexural strength $M_{u,cyc}$ of a steel column may be computed as follows,

$$\frac{M_{u,cyc}}{M_y^*} = 7{,}6\left(\frac{h_1}{t_w}\right)^{-0{,}4} \cdot \left(\frac{L_b}{i_z}\right)^{-0{,}16} \cdot (1-v_G)^{0{,}2} \leq 1{,}2 \quad (11)$$

$(R^2 = 0{,}87, COV = 0{,}07, N = 212 \text{ points})$

$$\theta_{u,cyc}^p = 7{,}37\left(\frac{h_1}{t_w}\right)^{-0{,}95} \cdot \left(\frac{L_b}{i_z}\right)^{-0{,}5} \cdot (1-v_G)^{2{,}4} \leq 0{,}15rad \quad (12)$$

$(R^2 = 0{,}86, COV = 0{,}38, N = 212 \text{ points})$

The equation is valid within the following range of parameters, $3{,}7 < h_1/t_w < 58$; $38 \leq L_b/i_z \leq 115$; $0 \leq v_G \leq 0{,}50$. Unlike monotonic loading, steel columns comprising cross-

sections with h_1/t_w<12 exhibit flexural strength deterioration due to the accumulated plastic strain from the imposed symmetric cyclic loading protocol.

Equations (10) and (12) exhibit fairly small variability as indicated by the associated COV and R^2 values. It is also found that $\theta^p_{u,mon}/\theta^p_{u,cyc} \cong 3{,}0$. The difference is attributed to the cumulative damage from inelastic loading cycles imposed to steel columns during a symmetric cyclic loading protocol contrary to the monotonic one. The above difference is deemed reasonable based on similar comparisons on steel and reinforced concrete members [51].

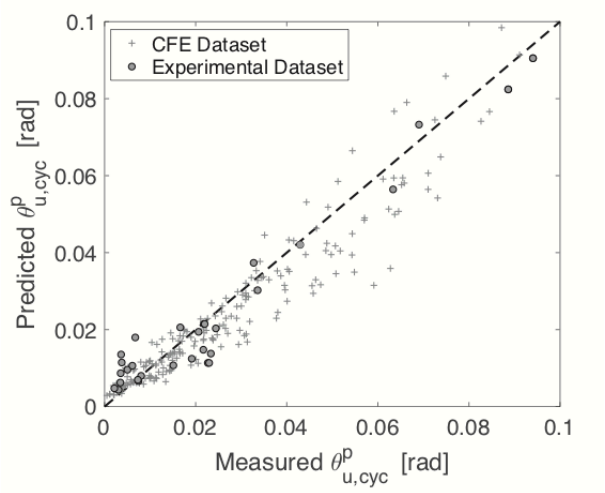

Figure 8 Comparison of measured and predicted responses for plastic rotation of steel columns from yield to ultimate

The sufficiency of the proposed formulations for predicting $\theta^p_{u,mon}$ and $\theta^p_{u,cyc}$ is also shown in Figure 8. The predicted $\theta^p_{u,cyc}$ values indicate a relatively good fit reflected by the data points clustered close to the dashed line. Reasonably good fit of the experimental dataset is notable because none of these data points were included in the development of the empirical equations. Same findings hold true for monotonic loading. The average error between the predicted and measured θ^p_u values is about 10% regardless of the loading type.

4.3 Effect of loading history on plastic rotation from yield to ultimate

Prior studies [15], [34], [52], [53] have questioned to what extent we should be conditioning the seismic performance and acceptance criteria of structures at incipient collapse based on envelope curves developed from symmetric cyclic loading histories. In this case, non-symmetric loading histories representing the ratcheting behaviour of structures prior to collapse are deemed to be more representative for quantifying the actual structural demands [33], [54]. Figure 9a shows such a comparison based on the moment-rotation relation of three nominally identical

steel columns subjected to monotonic, symmetric cyclic and collapse-consistent loading protocols from recent experiments by the first author [15]. Equations (10) and (12) are evaluated herein with an additional dataset of steel columns subjected to collapse-consistent loading histories [33]. Figure 9b depicts the $\theta^p_{u,mon}$ and $\theta^p_{u,cyc}$ versus h_1/t_w ratio. The computed values from Eqs (10) and (12) are normalized with respect to $\theta^p_{u,CPS}$ retrieved from the additional dataset. It is seen that $\theta^p_{u,cyc}$ is, on average, 50% less than that from a collapse-consistent protocol; whereas the corresponding value for the monotonic case is 1,2 times larger than $\theta^p_{u,CPS}$.

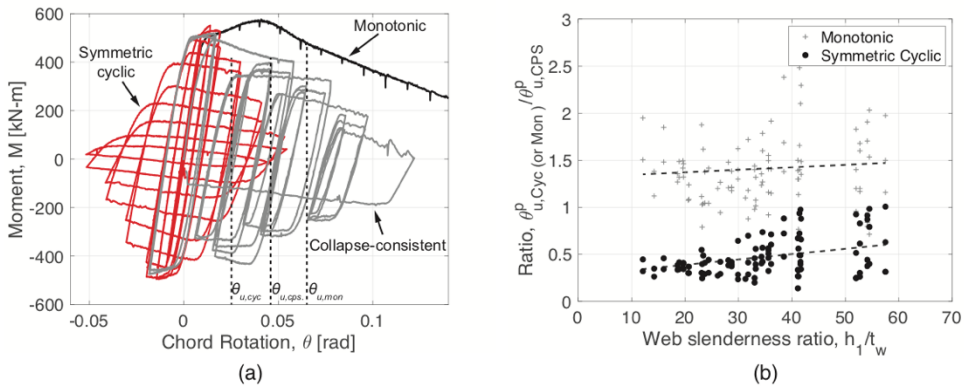

Figure 9 Influence of loading history on plastic rotation of steel columns from yield to ultimate (data from Suzuki and Lignos [15])

Therefore, if performance evaluation at incipient collapse is of interest, $\theta^p_{u,mon}$ may provide valuable information. Hence, a monotonic test is recommended in addition to cyclic ones for experimental evaluation of structural members at the near collapse limit state.

4.4 Assessment of EC8-Part 3 recommendations at near collapse limit state

Figure 10 illustrates a comparison between the current EC8-Part 3 modelling recommendations and the proposed ones according to Eq. (12) at near collapse limit state. Only test specimens with Class 1 and 2 cross-sections are employed in this comparison. Particularly, EC8-Part 3 suggests that Class 1 and 2 column cross-sections subjected to $\nu \leq 0{,}30$, regardless their geometric characteristics, exhibit ductilities at the NC limit state of $8 \cdot \theta_y$ and $3 \cdot \theta_y$, respectively. The figure suggests that the current EC8-Part 3 modelling recommendations overpredict by 20% to 30%, on average, $\theta^p_{u,cyc}$, in most cases that, $\nu \leq 0{,}30$; whereas in cases that $\nu > 0{,}30$ they significantly under predict the plastic rotation capacity of steel columns regardless of the employed cross-section classification. The above important observations are attributed to the fact that the EC8-Part3 modelling provisions neglect the dependence of $\theta^p_{u,cyc}$ on the geometric (web

and member slenderness ratio) and loading (axial load ratio) conditions of the respective column members. On the other hand, the proposed modelling recommendations trace the corresponding $\theta^{p}_{u,cyc}$ values with a noteworthy accuracy.

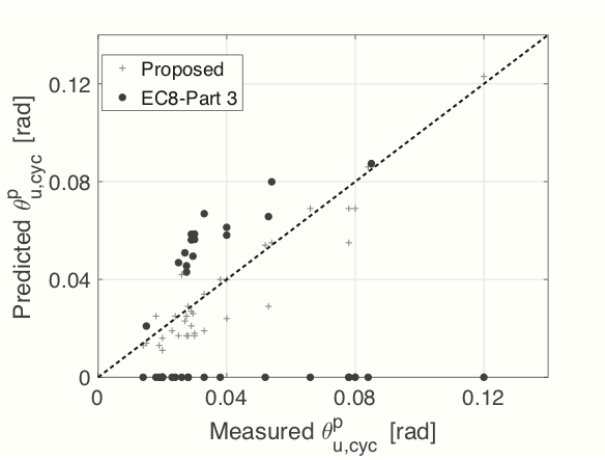

Figure 10 Comparison between proposed modelling recommendations and current EC8-Part 3 provisions at near collapse limit state

5 Conclusions and recommendations

This article discusses the development of practice-oriented nonlinear component models to compute the chord rotations and associated flexural strength of I- and H-shaped steel columns at yield and ultimate (near collapse) under monotonic and cyclic loading. The proposed models may be used within the future framework of Eurocode 8 Part 3 (EC8-Part 3) for the seismic performance assessment of new and existing steel structures based on nonlinear static (pushover) analysis. The models, which are based on collected experimental and simulated results from two assembled databases of steel columns, capture the main aspects of steel column response at yield and near collapse limit states. The former is relevant for repairability, whereas the latter is prevalent for collapse prevention evaluation.

The elastic rotational stiffness, K_e, of steel columns under combined axial load and lateral drift demands should consider both the flexural and shear contributions (Eqs. (2), (3) and (4)). It is shown that the effective flexural resistance, M_y^*, of steel columns may be estimated reasonably well based on the AISC-360-16 flexure – axial load interaction curve adjusted for the effects of material overstrength and hardening (see Eq. (6)). It is shown that the recommendation for no flexural resistance reduction according to EC3-Part 1 interaction curve, when the axial load ratio, $v \leq 0{,}25$, is not justifiable based on the gathered data.

The collected data underscore the influence of the shear span-to-depth ratio and axial load ratio

on the column chord rotations at yielding, θ_y. Both effects are depicted based on first principles of mechanics (see Eq. (6)). With regards to the ultimate chord rotation, θ_u, of steel columns (rotation at 20% column peak flexural strength drop), it should be computed based on the plastic rotation, θ_u^p, from yield to ultimate plus θ_y. For this reason, empirical expressions are developed for θ_u^p that capture the interrelation of the local slenderness ratio, h_1/t_w, the member slenderness ratio, L_b/i_z and the gravity-induced compressive axial load ratio, v_G for both monotonic (see Eq. (10)) and cyclic loading (see Eq. (12)). It is shown that the proposed expressions represent much better the available experimental and simulated data than the current EC8-Part 3 modelling recommendations for I- and H-shaped steel columns. Accordingly, expressions are provided for estimating the flexural strength, M_u, of columns at the ultimate chord rotation for monotonic (see Eq. (9)) and cyclic loading (see Eq. (11)).

Comprehensive comparisons with available data from steel columns under collapse-consistent loading histories suggest that their chord rotation at ultimate may be represented more rationally by the computed value based on monotonic loading (see Eq. (10)) reduced by about 20% to account for the influence of cumulative inelastic damage prior to incipient collapse. Thus, if performance at incipient collapse is of interest, a monotonic test should always be complementing the cyclic test data in future experimental studies.

Acknowledgements

This study is based on work supported by the Swiss National Science Foundation (Project No. 200021_188476). The financial support is gratefully acknowledged. The authors acknowledge Mr. Subash Ghimire (doctoral student at University of Grenoble, France, formerly research assistant at EPFL) and Dr. Ahmed Elkady (Lecturer at University of Southampton, UK, formerly Post-doc at EPFL) for assembling the databases that were used in this paper. Any opinions expressed in the paper are those of the authors and do not necessarily reflect the views of sponsors.

References

[1] FEMA, "Quantification of building seismic performance factors, Report FEMA-P695." Federal Emergency Management Agency (FEMA), Washington, DC, 2009.
[2] J. Žižmond and M. Dolšek, "The formulation of risk-targeted behaviour factor and its application to reinforced concrete buildings," in *16th World Conference of Earthquake Engineering*, Santiago, Chile, 2017, p. 12.
[3] P. Franchin, F. Petrini, and F. Mollaioli, "Improved risk-targeted performance-based seismic design of reinforced concrete frame structures," *Earthquake Engineering & Structural Dynamics*, vol. 47, no. 1, pp. 49–67, 2018.
[4] A. Elkady and D. G. Lignos, "Effect of gravity framing on the overstrength and collapse capacity of steel frame buildings with perimeter special moment frames," *Earthquake*

Engng Struct. Dyn., vol. 44, no. 8, pp. 1289–1307, Jul. 2015.
[5] ASCE, "Seismic evaluation and retrofit of existing buildings." American Society of Civil Engineers, Reston, Virginia, 2017.
[6] FEMA, "Improvement of nonlinear static seismic analysis procedures, Report FEMA 440." Federal Emergency Management Agency (FEMA), Washington, DC, 2005.
[7] CEN, "Eurocode 8: Design of structures for earthquake resistance - part 3: assessment and retrofitting of buildings," European Commitee for Standardization, Brussels, Belgium, Design Provisions Eurocode 8 Part 3, 2005.
[8] T. B. Panagiotakos and M. N. Fardis, "Deformations of reinforced concrete members at yielding and ultimate," *SJ*, vol. 98, no. 2, pp. 135–148, Mar. 2001.
[9] D. G. Lignos and H. Krawinkler, "Deterioration modeling of steel components in support of collapse prediction of steel moment frames under earthquake loading," *Journal of Structural Engineering*, vol. 137, no. 11, pp. 1291–1302, 2011.
[10] H. El Jisr, A. Elkady, and D. G. Lignos, "Composite steel beam database for seismic design and performance assessment of composite-steel moment-resisting frame systems," *Bull Earthquake Eng*, vol. 17, no. 6, pp. 3015–3039, Jun. 2019.
[11] A. Anastasiadis, V. Gioncu, and F. Mazzolani, "New trends in the evaluation of available ductility of steel members," in *Behaviour of Steel Structures in Seismic Areas*, Montreal, Canada, 2000.
[12] V. Gioncu and D. Petcu, "Available rotation capacity of wide-flange beams and beam-columns Part 1. Theoretical approaches," *Journal of Constructional Steel Research*, vol. 43, no. 1, pp. 161–217, Jul. 1997.
[13] M. Feldmann and M. Sedlacek, "Plastic ductility of I- and H-shaped beams subjected to static and dynamic loading," in *Stability and Ductility of Steel Structures (SDSS)*, Nagoya, Japan, 1997.
[14] C.-P. Lamarche and R. Tremblay, "Seismically induced cyclic buckling of steel columns including residual-stress and strain-rate effects," *Journal of Constructional Steel Research*, vol. 67, no. 9, pp. 1401–1410, Sep. 2011.
[15] Y. Suzuki and D. G. Lignos, "Large scale collapse experiments of wide flange steel beam-columns," in *8th International Conference on Behavior of Steel Structures in Seismic Areas (STESSA)*, Shanghai, China, 2015.
[16] G. Ozkula, J. Harris, and C.-M. Uang, "Observations from cyclic tests on deep, wide-flange beam-columns," *AISC Engineering Journal*, no. 1, p. 16, 2017.
[17] G. Toutant, Y. B. Minouei, A. Imanpour, S. Koboevic, and R. Tremblay, "Stability of steel columns in steel concentrically braced frames subjected to seismic loading," in *Structures Congress 2017*, Denver, Colorado, USA, 2017.
[18] A. Elkady and D. G. Lignos, "Full-scale testing of deep wide-flange steel columns under multiaxis cyclic loading: Loading sequence, boundary effects, and lateral stability bracing force demands," *ASCE Journal of Structural Engineering*, vol. 144, no. 2, pp. 04017189-1–15, 2018.
[19] J. Cravero, A. Elkady, and D. G. Lignos, "Experimental evaluation and numerical modeling of wide-flange steel columns subjected to constant and variable axial load coupled with lateral drift demands," *ASCE Journal of Structural Engineering*, vol. (accepted for publication), 2019.
[20] A. Elkady and D. G. Lignos, "Analytical investigation of the cyclic behavior and plastic hinge formation in deep wide-flange steel beam-columns," *Bull Earthquake Eng*, vol. 13, no. 4, pp. 1097–1118, Jun. 2015.
[21] A. Elkady and D. Lignos G., "Improved seismic design and nonlinear modeling recommendations for wide-flange steel columns," *Journal of Structural Engineering*, vol. 144, no. 9, p. 04018162, Sep. 2018.
[22] CEN, "Eurocode 8, Design of structures for earthquake resistance - Part 1: General rules, seismic actions and rules for buildings," European Committee for Standardization (CEN), Brussels, Design Provisions Eurocode 8, Part 1-1, 2005.
[23] Y. Suzuki and D. G. Lignos, "Fiber-based model for earthquake-induced collapse simulation of steel frame buildings," in *Eleventh U.S. National Conference on Earthquake Engineering*, Los Angeles, CA, USA, 2018.
[24] CEN, "Design of steel structures - Eurocode 3, Part 1-1: General rules and rules for buildings," European Committee for Standardization (CEN), Brussels, Design Provisions Eurocode 3, Part 1-1, 2005.
[25] E. Popov, V. V. Bertero, and S. Chandramouli, "Hysteretic behavior of steel columns," Earthquake Engineering Research Center, University of California, Berkeley, California, UCB/EERC-75/11, 1975.
[26] G. A. MacRae, A. J. Carr, and W. R. Walpone, "The seismic response of steel frames," Department of Civil Engineering, University of Canterbury, Christchurch, New Zealand,

PhD Thesis 90–6, 1990.
[27] M. Nakashima, K. Takanashi, and H. Kato, "Test of steel beam-columns subject to sidesway," *Journal of Structural Engineering*, vol. 116, no. 9, pp. 2516–2531, 1990.
[28] J. Newell and C.-M. Uang, "Cyclic behavior of steel wide-flange columns subjected to large drift," *Journal of Structural Engineering*, vol. 134, no. 8, pp. 1334–1342, 2008.
[29] X. Cheng, Y. Chen, and L. Pan, "Experimental study on steel beam–columns composed of slender H-sections under cyclic bending," *Journal of Constructional Steel Research*, vol. 88, pp. 279–288, Sep. 2013.
[30] X. Cheng, Y. Chen, and D. A. Nethercot, "Experimental study on H-shaped steel beam-columns with large width-thickness ratios under cyclic bending about weak-axis," *Engineering Structures*, vol. 49, pp. 264–274, Apr. 2013.
[31] C. Chen, C. Wang, and H. Sun, "Experimental study on seismic behavior of full encased steel-concrete composite columns," *Journal of Structural Engineering*, vol. 140, no. 6, p. 04014024, 2014.
[32] H. Krawinkler, "Cyclic loading histories for seismic experimentation on structural components," *Earthquake Spectra*, vol. 12, no. 1, pp. 1–12, Feb. 1996.
[33] Y. Suzuki and D. G. Lignos, "Development of collapse-consistent loading protocols for experimental testing of steel columns," *Earthquake Engineering & Structural Dynamics (accepted)*, 2019.
[34] D. G. Lignos, H. Krawinkler, and A. S. Whittaker, "Prediction and validation of sidesway collapse of two scale models of a 4-story steel moment frame," *Earthquake Engng. Struct. Dyn.*, vol. 40, no. 7, pp. 807–825, Jun. 2011.
[35] D. G. Lignos, T. Hikino, Y. Matsuoka, and M. Nakashima, "Collapse assessment of steel moment frames based on E-Defense full-scale shake table collapse tests," *Journal of Structural Engineering*, vol. 139, no. 1, pp. 120–132, 2013.
[36] E. Voce, "The relationship between stress and strain for homogeneous deformation," *Journal of the Institute of Metals*, vol. 74, pp. 537–562, 1948.
[37] P. J. Armstrong and C. O. Frederick, "A mathematical representation of the multiaxial bauschinger effect," Berkeley Nuclear Laboratories, Berkeley, California, Technical Report RD/B/N 731, 1966.
[38] J. L. Chaboche, "Constitutive equations for cyclic plasticity and cyclic viscoplasticity," *International Journal of Plasticity*, vol. 5, no. 3, pp. 247–302, Jan. 1989.
[39] A. C. Sousa and D. G. Lignos, "On the inverse problem of classic nonlinear plasticity models-An application to cyclically loaded structural steels," Resilient Steel Structures Laboratory (RESSLab), Ecole Polytechnique Fédérale de Lausanne, Lausanne, Technical Report No. 231968 231968, 2017.
[40] A. Hartloper, A. C. Sousa, and D. G. Lignos, "Sensitivity of simulated steel column instabilities to plasticity model assumptions," in *12th Canadian Conference on Earthquake Engineering*, Quebec, Canada, 2019.
[41] R. J. Cooke and A. M. Kanvinde, "Constitutive parameter calibration for structural steel: Non-uniqueness and loss of accuracy," *Journal of Constructional Steel Research*, vol. 114, pp. 394–404, Nov. 2015.
[42] B. W. Young, "Residual stresses in hot-rolled sections," in *International Colloquium on Column Strength*, Zurich, Switzerland, 1971, pp. 25–38.
[43] A. C. Sousa and D. G. Lignos, "Residual stress measurements of European hot-rolled I-shaped steel profiles," École Polytechnique Fédérale de Lausanne (EPFL), Lausanne, Switzerland, 231302, Oct. 2017.
[44] EN 10024, "Hot rolled taper flange I sections - tolerances on shape and dimensions." Comite Europeen de Normalisation, 1995.
[45] G. R. Cowper, "The shear coefficient in Timoshenko's beam theory," *ASME Journal of Applied Mechanics*, pp. 335–340, 1966.
[46] AISC, "Specification for structural steel buildings, ANSI/AISC 360-16," American Institute for Steel Construction, Chicago, IL, Seismic Provisions ANSI/AISC 360-16, 2016.
[47] A. Braconi, M. Finetto, and H. Degee, "Optimizing the seismic performance of steel and and steel-concrete structures by standardizing material quality control (OPUS)," European Commission, Luxumbourg, 2013.
[48] R. Landolfo *et al.*, "Equaljoints PLUS Volume with information brochures for 4 seismically qualified joints," European Convention for Construction Steelwork, Coimbra, Portugal, EQJ1-EN, 1st Edition, 2018.
[49] D. G. Lignos, A. R. Hartloper, A. Elkady, G. G. Deierlein, and R. Hamburger, "Proposed updates to the ASCE 41 nonlinear modeling parameters for wide-flange steel columns in support of performance-based seismic engineering," *Journal of Structural Engineering*, vol. 145, no. 9, p. 04019083, Sep. 2019.
[50] C. B. Haselton, A. B. Liel, S. T. Lange, and G. G. Deierlein, "Beam-Column element model

calibrated for predicting flexural response leading to global collapse of RC frame buildings," Pacific Earthquake Engineering Research Center (PEER), Berkeley, CA, USA, 2007/03, 2008.

[51] NIST, "Recommended modeling parameters and acceptance criteria for nonlinear analysis in support of seismic evaluation, retrofit, and design," National Institute of Standards and Technology, Gaithersburg, MD, NIST GCR 17-917-45, Apr. 2017.

[52] H. Krawinkler, "Loading histories for cyclic tests in support of performance assessment of structural components," in *3rd International Conference on Advances in Experimental Seismic Engineering*, San Francisco, California, 2009.

[53] B. F. Maison and M. S. Speicher, "Loading protocols for ASCE 41 backbone curves," *Earthquake Spectra*, vol. 32, no. 4, pp. 2513–2532, Aug. 2016.

[54] A. Nojavan, A. E. Schultz, C. Haselton, S. Simathathien, X. Liu, and S.-H. Chao, "A new data set for full-scale reinforced concrete columns under collapse-consistent loading protocols," *Earthquake Spectra*, vol. 31, no. 2, pp. 1211–1231, Mar. 2015.

Authors of this paper:

Prof. Dr.-Ing. Dimitrios G. Lignos

École Polytechnique Fédérale de Lausanne,

Civil Engineering Institute, IIC

EPFL, Resilient Steel Structures Laboratory, GC B3 485, Station 18

1015, Lausanne, Switzerland

dimitrios.lignos@epfl.ch

Mr.-Ing. Alexander R. Hartloper

École Polytechnique Fédérale de Lausanne,

Civil Engineering Institute, IIC

EPFL, Resilient Steel Structures Laboratory, GC B3 524, Station 18

1015, Lausanne, Switzerland

alexander.hartloper@epfl.ch

Kommentare